

5-20-2014

Quantifying the Influence of Deep Soil Moisture on Ecosystem Albedo: The Role of Vegetation

Zulia Mayari Sanchez-Mejia
University of Arizona

Shirley Anne Papuga
University of Arizona, shirley.papuga@wayne.edu

Jessica Blaine Swetish
University of Arizona

Willem Jan Dirk van Leeuwen
University of Arizona

Daphne Szutu
University of Arizona

See next page for additional authors

Follow this and additional works at: <https://digitalcommons.wayne.edu/geofrp>

 Part of the [Environmental Sciences Commons](#)

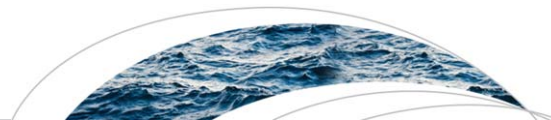
Recommended Citation

Sanchez-Mejia, Z. M., S. A. Papuga, J. B. Swetish, W. J. D. van Leeuwen, D. Szutu, and K. Hartfield (2014), Quantifying the influence of deep soil moisture on ecosystem albedo: The role of vegetation, *Water Resour. Res.*, 50, 4038–4053, doi:[10.1002/2013WR014150](https://doi.org/10.1002/2013WR014150).

This Article is brought to you for free and open access by the Environmental Sciences and Geology at DigitalCommons@WayneState. It has been accepted for inclusion in Environmental Science and Geology Faculty Research Publications by an authorized administrator of DigitalCommons@WayneState.

Authors

Zulia Mayari Sanchez-Mejia, Shirley Anne Papuga, Jessica Blaine Swetish, Willem Jan Dirk van Leeuwen, Daphne Szutu, and Kyle Hartfield



RESEARCH ARTICLE

10.1002/2013WR014150

Key Points:

- Semiarid ecosystem greenness is triggered by deep soil moisture
- Deep soil moisture decreases canopy albedo
- Deep soil moisture is important in semiarid land-atmosphere interactions

Correspondence to:

S. A. Papuga,
papuga@email.arizona.edu

Citation:

Sanchez-Mejia, Z. M., S. A. Papuga, J. B. Swetish, W. J. D. van Leeuwen, D. Szutu, and K. Hartfield (2014), Quantifying the influence of deep soil moisture on ecosystem albedo: The role of vegetation, *Water Resour. Res.*, 50, 4038–4053, doi:10.1002/2013WR014150.

Received 20 MAY 2013

Accepted 22 APR 2014

Accepted article online 25 APR 2014

Published online 20 MAY 2014

Quantifying the influence of deep soil moisture on ecosystem albedo: The role of vegetation

Zulia Mayari Sanchez-Mejia¹, Shirley Anne Papuga¹, Jessica Blaine Swetish¹, Willem Jan Dirk van Leeuwen^{1,2}, Daphne Szutu¹, and Kyle Hartfield¹

¹School of Natural Resources and the Environment, University of Arizona, Tucson, Arizona, USA, ²School of Geography and Development, University of Arizona, Tucson, Arizona, USA

Abstract As changes in precipitation dynamics continue to alter the water availability in dryland ecosystems, understanding the feedbacks between the vegetation and the hydrologic cycle and their influence on the climate system is critically important. We designed a field campaign to examine the influence of two-layer soil moisture control on bare and canopy albedo dynamics in a semiarid shrubland ecosystem. We conducted this campaign during 2011 and 2012 within the tower footprint of the Santa Rita Creosote Ameriflux site. Albedo field measurements fell into one of four Cases within a two-layer soil moisture framework based on permutations of whether the shallow and deep soil layers were wet or dry. Using these Cases, we identified differences in how shallow and deep soil moisture influence canopy and bare albedo. Then, by varying the number of canopy and bare patches within a gridded framework, we explore the influence of vegetation and soil moisture on ecosystem albedo. Our results highlight the importance of deep soil moisture in land surface-atmosphere interactions through its influence on aboveground vegetation characteristics. For instance, we show how green-up of the vegetation is triggered by deep soil moisture, and link deep soil moisture to a decrease in canopy albedo. Understanding relationships between vegetation and deep soil moisture will provide important insights into feedbacks between the hydrologic cycle and the climate system.

1. Introduction

Land surface characteristics strongly influence the energy and water dynamics and exchange with the atmosphere [e.g., Gu *et al.*, 2007]. In arid and semiarid environments, land surface changes associated with shrub encroachment [e.g., Asner *et al.*, 2003; Grover and Musick, 1990; Van Auken, 2000] or desertification [e.g., Carrion *et al.*, 2010; Otterman, 1974] include major changes in their characteristic complex mosaic of vegetation [Archer, 1990; Ge and Zou, 2013]. Furthermore, soil moisture drives vegetation patterns [Seghier *et al.*, 1997], for instance by creating circumstances in which woody species can exploit moisture heterogeneity [Austin *et al.*, 2004; Moody and Meentemeyer, 2001; Partel and Helm, 2007].

Due to the strong linkage between soil moisture and vegetation, soil-plant-atmosphere feedbacks can be especially dynamic in space and time in dryland ecosystems [Niyogi *et al.*, 1999; Philippon *et al.*, 2005; Rodriguez-Iturbe, 2000; Rodriguez-Iturbe *et al.*, 1999]. For instance, changes in precipitation and frequency influence plant available moisture, which has an impact on vegetation cover [Nicholson, 2000; Thomey *et al.*, 2011]. Furthermore, vegetation cover, type, and phenology can exert a strong influence on the radiation budget [e.g., Villegas *et al.*, 2010a]. Because the radiation budget drives surface energy dynamics, changes in precipitation dynamics are expected to result in modified land-surface atmosphere interactions through these vegetation feedbacks [Overpeck and Udall, 2010].

One way that vegetation influences surface energy fluxes and atmospheric dynamics is through altering the albedo of the land surface [Baldocchi *et al.*, 2004; Otterman, 1977; Song, 1999; Swann *et al.*, 2012]. Generally speaking, landscapes with sparse vegetation cover tend to have higher albedo than more vegetated landscapes [Charney, 1975; Nicholson *et al.*, 1998; Roberts *et al.*, 2004], owing to the extensive bare soil. However, the temporal variability of albedo is especially dynamic in semiarid and arid regions because the phenology of the vegetation is strongly linked to moisture inputs [Huxman *et al.*, 2004; Reynolds *et al.*, 1999; Robinove *et al.*, 1981; Song, 1999]. For instance, surface albedo of semiarid ecosystems has been shown to be lower during the wet season due to an increase in leaf area index and greenness of the vegetation [Colwell, 1974; Wang *et al.*, 2007]. Further, remote sensing observations in semiarid ecosystems have also shown a decrease

in albedo during the monsoon season that is associated with an increase in vegetation greenness [Liang *et al.*, 2005; Mendez-Barroso *et al.*, 2009; Wu *et al.*, 1995].

In drylands, small frequent precipitation events moisten the surface layer of the soil [Sala and Lauenroth, 1982]. This moisture darkens the color of the soil surface [Lobell and Asner, 2002; Wang *et al.*, 2011], consequently decreasing land surface albedo after these small storms [Duchon and Hamm, 2006; Small and Kurc, 2003]. Large infrequent precipitation events in these regions are capable of wetting the deeper soil layer [Huxman *et al.*, 2004; Kurc and Small, 2007; Schwinnig and Sala, 2004]. This deep moisture triggers vegetation processes [Grover and Musick, 1990; Noy-Meir, 1973] and leads to a green-up of the shrub canopy [Kurc and Benton, 2010]. Greening and thickening of canopy foliage have been shown to decrease albedo [Zhang *et al.*, 2013; Zhang and Walsh, 2006]. Therefore, large precipitation events and the subsequent wetting of deep soil layers are likely to influence ecosystem albedo in arid and semiarid regions.

Different plant functional types allocate roots to different soil depths (shallow or deep) for water access [Asbjornsen *et al.*, 2011; Jackson *et al.*, 2000; Loik *et al.*, 2004]. Because of this layered root allocation, ecosystems are often considered to be comprised of both shallow-rooted and deep-rooted plants, a hypothetical two-layer strategy for minimizing competition for moisture and other resources [Mahrt and Pan, 1984; Walter, 1972; Wiegand *et al.*, 2006]. Because certain plants in arid and semiarid ecosystems can access longer lasting water from deeper soil layers [Kurc and Small, 2007; Raz-Yaseef *et al.*, 2012], there is growing interest in the effects of this deep moisture on surface and atmospheric processes [Basara and Crawford, 2002; Siqueira *et al.*, 2009], especially as they relate to albedo [Sanchez-Mejia and Papuga, 2014; Santanello *et al.*, 2009; Zaitchik *et al.*, 2013].

The aim of this research is to identify differences in how shallow and deep soil moisture influence ecosystem albedo through modifying aboveground characteristics of the vegetation, such as greenness. We demonstrate that changes in vegetation due to deep soil moisture availability result in changes in albedo, thereby linking deep soil moisture and albedo. We do this by modifying a simple two-layer soil moisture conceptual framework of four Cases: (1) a dry shallow layer (0–20 cm) with a dry deep layer (20–60 cm), (2) a wet shallow layer with a dry deep layer, (3) a wet shallow layer with a wet deep layer, and (4) a dry shallow layer with a wet deep layer [Sanchez-Mejia and Papuga, 2014]. For the purposes of this study, we evaluate each Case for a bare patch and for a shrub patch (Figure 2). We hypothesize that decreasing deep soil moisture (Cases 1 and 2) will result in a dry and light-colored canopy (Figure 2a), while increasing soil moisture in the deep layer (Cases 3 and 4) will result in a wet and dark-colored (greener) canopy (Figure 2a). We further hypothesize that a dry land surface, either through dry shallow soil (Case 1 bare and Case 4 bare; Figure 2) or through dry vegetation (Case 1 canopy and Case 2 canopy; Figure 2) should increase overall ecosystem albedo. Alternatively, a wet land surface, either through wet shallow soil (Case 2 bare and Case 3 bare; Figure 2) or through darker (greener) vegetation (Case 3 canopy and Case 4 canopy; Figure 2) should decrease overall ecosystem albedo. Using this framework, we demonstrate the role of deep soil moisture on land surface-atmosphere interactions through its influence on vegetation.

2. Study Area and Methods

2.1. Site Description

The study site is located within a 250 m footprint of an eddy covariance (EC) tower located in a creosotebush-dominated ecosystem on the Santa Rita Experimental Range (SRER; Figure 1), approximately 25 km south of Tucson, Arizona [Kurc and Benton, 2010; Sanchez-Mejia and Papuga, 2014]. In addition to typical water and carbon fluxes, incident and reflected solar radiation are measured 10 m from the EC tower at 2.75 m above the surface with a four-component net radiometer (CNR1, Kipp & Zonen, Inc., Delft, the Netherlands). Because this is a relatively homogeneous landscape, the area measured by the radiometer is assumed to be representative of the EC footprint [Lucht *et al.*, 2000; Small and Kurc, 2003]. Six soil moisture profiles are also monitored at the EC tower with water content reflectometers (CS616, Campbell Scientific Inc., Logan, UT) at five different depths (2.5, 12.5, 22.5, 37.5, and 52.5 cm) in three bare and three shrub canopy sites. Additionally, within the footprint of this EC tower are three time-lapse digital cameras (phenocams) used to monitor plant phenology [Kurc and Benton, 2010].

Long-term annual average precipitation for the closest rain gage is 260 mm (Santa Rita Experimental Range Digital Database; <http://ag.arizona.edu/SRER/data.html>). According to these data, most of the rain occurs in

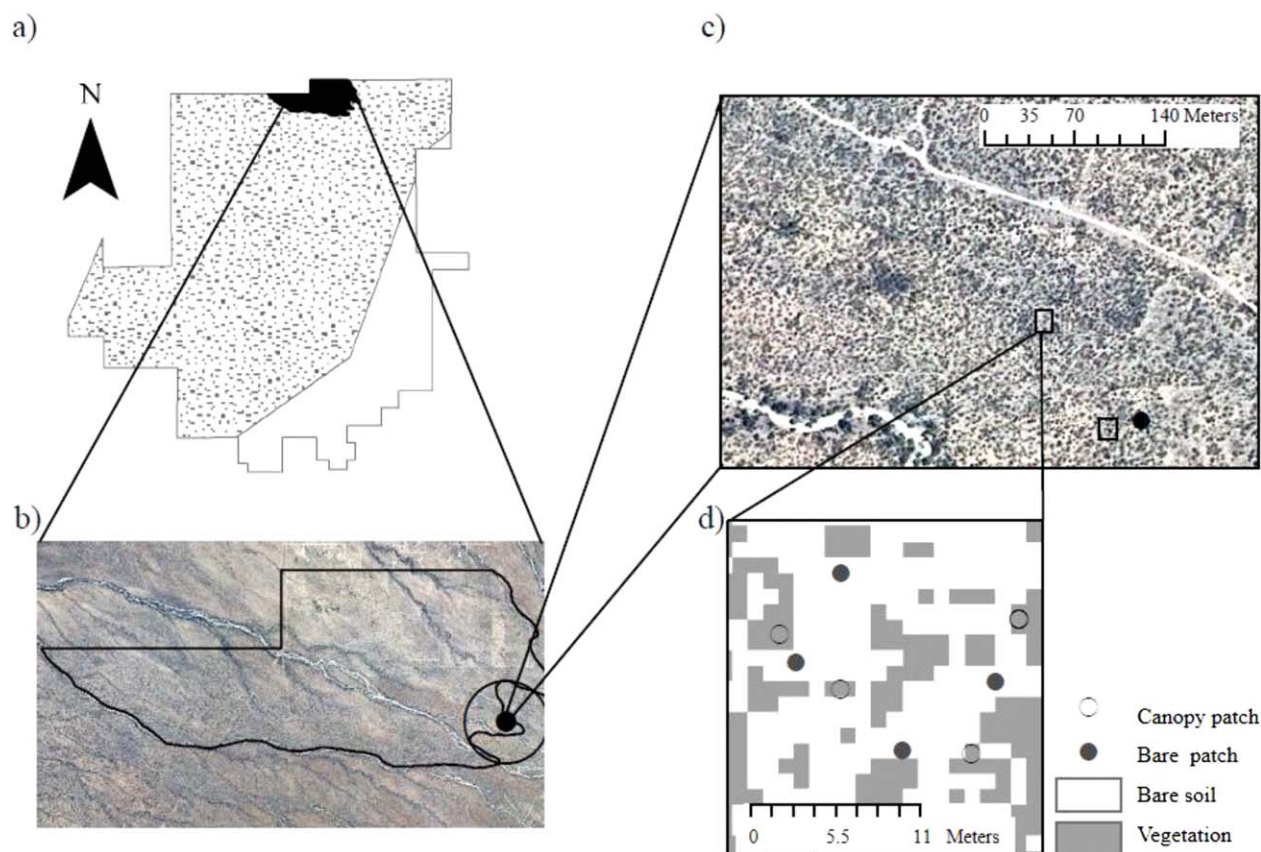


Figure 1. (a) The Santa Rita Experimental Range (SRER) boundary is shown in black, creosotebush (*L. tridentata*) distribution is shown with dotted gray, and black polygon indicates area where creosotebush dominates. (b) NAIP (National Agriculture Imagery Program, 2010) for the region showing flux tower with black dot and fetch area represented with a circle. (c) Close up to show sampling sites in black hollow squares. (d) Classified NAIP image with bare and canopy patches.

July, August, and September (~60%), while winter rains that occur in December, January, and February account for much less (~20%). Mean annual surface temperature is ~20°C, with monthly mean temperatures ranging from ~10°C during the winter to ~35°C during the summer.

Vegetation cover at the site is about 24%, from which 14% is creosotebush (*Larrea tridentata*) and nearly 10% is herbaceous cover and cacti [Kurc and Benton, 2010]. The topography is relatively flat (slopes < 2%), and the soil texture is sandy loam [Kurc and Benton, 2010], with a 10% increase of clay and silt from 35 to 75 cm depth (unpublished data from a 2008 laser diffraction particle size analysis) [Arriaga et al., 2006]. The root profiles show vertical and horizontal heterogeneity similar to what has been described in a conceptual model for shallow-extracting woody plants [Breshears and Barnes, 1999]; root density under bare patches is highest at 10 and at 35 cm depth, while under the canopy it is highest at 25 cm depth [Sanchez-Mejia and Papuga, 2014].

2.2. Field Campaign

Field campaigns were conducted in 2011 and 2012 to assess the influence of deep soil moisture on albedo of bare and vegetated patches. The soil profile was analyzed using a two-layer conceptual framework where the surface (0–20 cm) and deep (20–60 cm) layers can differ in moisture content (Figure 2a) [Sanchez-Mejia and Papuga, 2014]. Over a 2 year period, albedo measurements were made at eight bare and eight vegetated patches (Figure 1d) on four different occasions (Figure 3c) in each of the Cases.

To sample Case 1 (dry/dry), measurements were obtained during dry periods in which no precipitation events were recorded for at least 2 months (Figure 3a). To sample Case 2 (wet/dry), measurements were taken just after small precipitation events (<8 mm), so that the shallow layer would be wet but the deep layer would be dry. To sample Case 3 (wet/wet), measurements were taken just after large precipitation

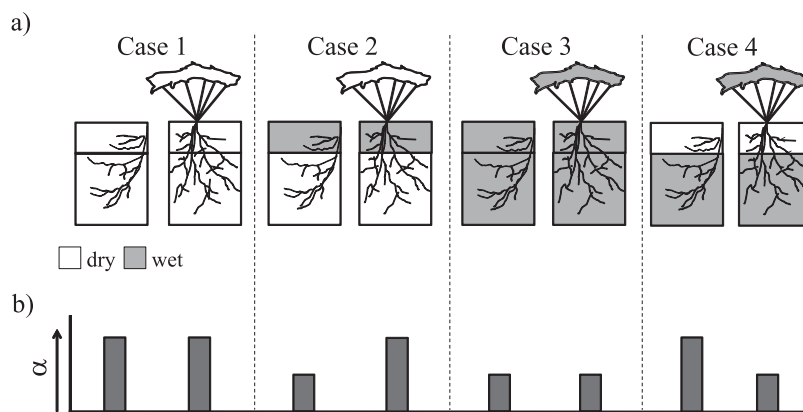


Figure 2. (a) The four Cases of the two-layer soil moisture conceptual framework broken into bare and canopy patches. Gray coloring represents wet and dark land surface and white coloring represents dry and light land surface. (b) The expected relative magnitude of albedo associated with bare and canopy patches for each Case.

events (>8 mm), so that both the shallow and deep layers would be wet. And finally, to sample Case 4 (dry/wet), measurements were taken several days (~4) after the large precipitation events used in Case 3. Real-time data from the nearby Sahuarita High School meteorological station (<http://sahuarita.cals.arizona.edu>) located 13 km from the EC tower site were used to track precipitation events.

We verified that our sampling days matched the soil moisture condition for each Case by using the soil moisture profile data (Figure 3b). Shallow (0–20 cm) and deep (20–60 cm) moisture were calculated using weighted averages of probes (with a source area radius of 7.5 cm) within each layer [Sanchez-Mejia and Papuga, 2014]. The amount of shallow or deep moisture contributing to the measurement by each probe was calculated using the equations below:

$$\theta_{\text{shallow}} = 0.33\theta_{2.5} + 0.5\theta_{12.5} + 0.17\theta_{22.5} \tag{1}$$

$$\theta_{\text{deep}} = 0.25\theta_{22.5} + 0.375\theta_{37.5} + 0.375\theta_{52.5} \tag{2}$$

We then used the thresholds established in Sanchez-Mejia and Papuga [2014] to determine in hindsight the actual Case status for each sampling period.

Similar to methods used in studies aimed at evaluating the characteristic timescales of the evaporation response in land surface models [Lohmann and Wood, 2003; Scott et al., 1997], we modeled the decrease in soil moisture in the shallow layer and in the deep layer as an exponential relationship through time [Hunt et al., 2002; Kurc and Small, 2004]:

$$\theta(t) = (\theta_1 - \theta_f)e^{-t/\tau} + \theta_f \tag{3}$$

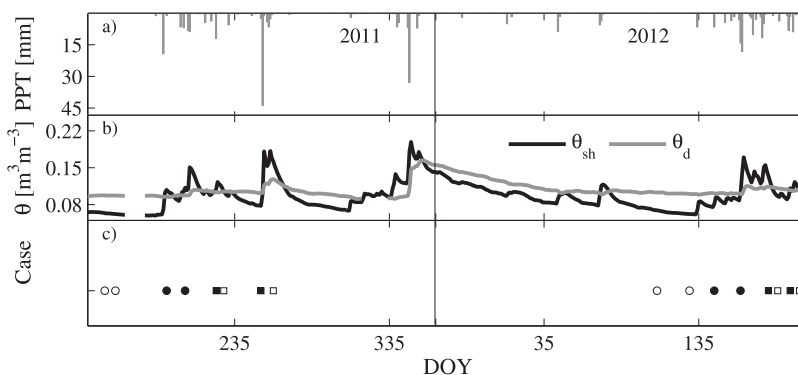


Figure 3. Time series (2011–2012) of (a) precipitation, (b) shallow (black line) and deep (gray line) soil moisture, and (c) day on which the field campaign was conducted for each Case (Case 1, open circles; Case 2, filled circles; Case 3, filled squares; and Case 4, open squares).

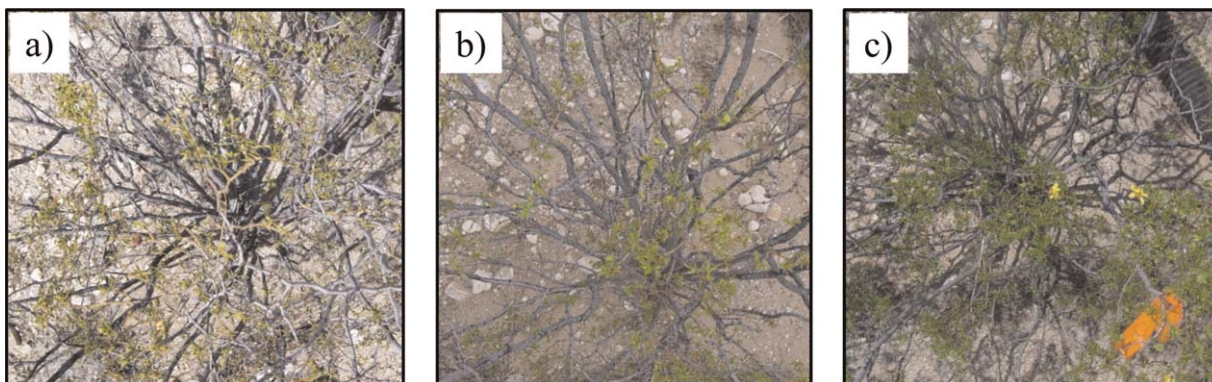


Figure 4. Examples of images taken during the field campaigns at each shrub where albedo was measured for (a) Case 1, (b) Case 2, and (c) Case 3. Images for Case 4 are missing and therefore not included here.

where θ is volumetric soil moisture ($\text{m}^3 \text{m}^{-3}$), t is the number of days since the rainfall event, θ_1 is the soil moisture observed on the first day following the rainfall event, θ_f is the soil moisture on the last day of the drydown, and τ is a best fit exponential time constant. We only used large storms (>8 mm) in our analysis.

2.2.1. Sampling Design

Measurements were made at two locations within the EC tower footprint, approximately 120 m apart. The first sampling site was approximately 100 m northwest of the tower and the second 20 m southwest of the tower (Figure 1c). We made measurements at four shrub canopy and four bare soil patches at each sampling site, for a total of eight shrub canopy patches and eight bare ground patches. At each patch, we measured reflected shortwave radiation twice during a 5 min time period between 12:00 and 2:00 P.M., when incoming shortwave radiation is maximized, using an Eppley PSP Precision Spectral Pyranometer (The Eppley Laboratory, Inc., Newport, RI) attached to a tripod and connected to a CR10X datalogger (Campbell Scientific, Inc., Logan, UT). The tripod was oriented so that the sensor was 0.3 m above the canopy of each shrub and 0.3 m above the ground level of each bare patch. The height of the sensor ensured that the majority of the source area for the measurement was directly from the feature of interest, thereby specifying a patch scale of <1.5 m in radius [Cescatti *et al.*, 2012; Schaaf *et al.*, 2011]. Note that incoming solar radiation values were obtained from the CNR1 at the tower location (see section 2.1).

In addition to shortwave radiation measurements, we also made qualitative measurements at each patch. Downward looking photos above canopy patches (Figure 4) and bare patches were taken to follow changes in leaf color and abundance and bare ground color. We also recorded visually ascertained leaf, branch, and soil color, and presence or absence of blooms, flowers, seed pods, and litter (Table 1).

2.2.2. Calculations

Ecosystem albedo was calculated as an average from 30 min measurements of incoming and outgoing shortwave radiation made between 10:00 A.M. and 2:00 P.M. at the EC tower for days aligning with the field campaign. Bare and canopy albedo values were calculated as $\alpha = SW_{\text{out}}/SW_{\text{in}}$ using the incoming shortwave

Table 1. Qualitative Data Generated From the Field Campaign^a

	Case 1	Case 2	Case 3	Case 4
<i>Canopy patches</i>				
Leaf color	Yellow-brown	Light green	Dark green	Dark green
Branch color	Light gray	Dark gray	Dark gray	Medium gray
Blooms	0/8	2/8	8/8	3/8
Flowers	0/8	0/8	8/8	6/8
Seed pods	2/8	3/8	4/8	7/8
<i>Bare patches</i>				
Soil color	Light brown	Brown	Brown	Light brown
Litter	2/8	5/8	5/8	7/8

^aBloom, flower, seed pod, and litter characteristics are presented as a fraction of the number of patches with the given characteristic, where $n = 8$ for both canopy and bare patches.

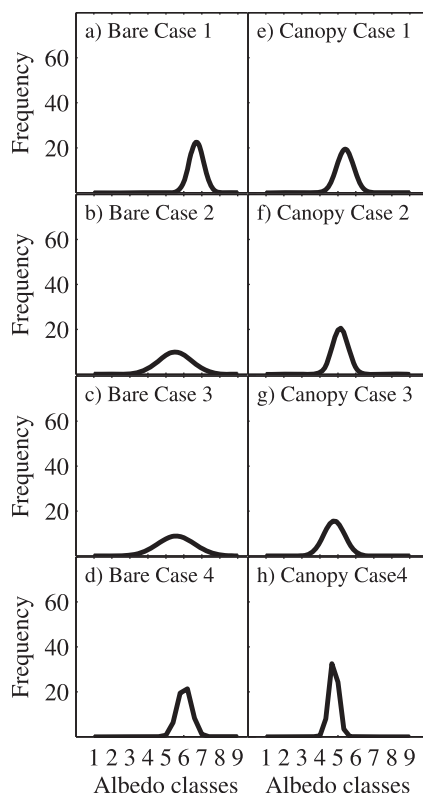


Figure 5. Probability distribution functions (PDFs) for albedo derived from field campaign measurements over bare and canopy patches for each Case: (a) Case 1, bare; (b) Case 2, bare; (c) Case 3, bare; (d) Case 4, bare; (e) Case 1, canopy; (f) Case 2, canopy; (g) Case 3, canopy; and (h) Case 4, canopy. Albedo class intervals are defined as 1 (<0.12), 2 (0.12–0.14), 3 (0.14–0.16), 4 (0.16–0.18), 5 (0.18–0.20), 6 (0.20–0.22), 7 (0.22–0.24), 8 (0.24–0.26), and 9 (>0.26).

radiation (SW_{in} [$W m^{-2}$]) from the EC tower and the reflected shortwave radiation (SW_{out} [$W m^{-2}$]) from the field campaign measurements. To match the 30 min EC data, we used an average of the two measurements taken in the 5 min time period within that 30 min period as the half hour SW_{out} and then calculated an albedo for that half hour to represent the daily albedo. The eight bare measurements were pooled together and then averaged to obtain a representative bare albedo, as were the eight canopy measurements to obtain a representative canopy albedo.

2.2.3. Virtual Landscape

Field campaign albedo measurements (4 days \times 8 locations \times 2 samples in time = 64 total values) were used to generate probability distribution functions (PDFs) for bare and canopy patches describing the frequency of albedo values around the mean for each Case (Figure 5), using a normal distribution; albedo classes were used to enhance comparison between Cases. We then used these PDFs in a simple virtual landscape in which each 1 m cell of a 100×100 m grid was populated with either a bare (0) or canopy (1) patch [Baldocchi *et al.*, 2005]. Albedos for each patch were assigned based on the PDFs. In this virtual landscape, vegetation cover can be modified and bare and canopy albedo values are coupled to the landscape. For our study, we increased cover from 0 to 100% (Figure 6) and then calculated ecosystem albedo as a function of vegetation cover for each soil moisture Case, i.e.:

$$\alpha_e(v) = \sum [(1-f)\alpha_b + f\alpha_c] \quad (4)$$

where α_e is ecosystem albedo, f is the percent canopy, α_b is bare albedo, and α_c is canopy albedo. Here, percent canopy f ranges from 0 to 1, determined by the outline of the shrubs, even when they are very sparse and bare soil is visible from above through the branches and leaves. Similarly, we assumed that a grid cell was either completely covered by a shrub (canopy) or completely uncovered (bare), i.e., a sparse canopy patch would not influence the grid differently than a full canopy patch. While this assumption is a simplification of canopy architecture and vegetation composition, it is a starting point that can eventually be strengthened with a dynamic vegetation model [e.g., Bonan *et al.*, 2003; Krinner *et al.*, 2005]. With this model, we can investigate the influence of vegetation cover on albedo with respect to moisture in the shallow or deep soil layers.

2.3. Camera-Derived Greenness

The three pheno-cams were originally placed to account for different sizes and aggregate structure of the creosotebush community within the footprint of the EC tower. The digital cameras (Moultrie Game Spy I-60) were mounted on poles at 1 m (lens-to-ground distance), oriented with a field-of-view parallel to the ground surface, facing northward to maximize sunlight and to minimize shading [Kurc and Benton, 2010].

Regardless of cloud cover, the daily solar noon image from each camera was analyzed for greenness by utilizing a constant rectangular region of interest (ROI) [Richardson *et al.*, 2007], approximately 400×2800 pixels, selected to maximize creosotebush density by integrating several individuals within each image [Kurc and Benton, 2010]. Each ROI was then analyzed for greenness I_g using the following relationship developed by Richardson *et al.* [2007] for a deciduous broadleaf forest which has also been demonstrated to be effective in sparse evergreen shrublands [Kurc and Benton, 2010]:

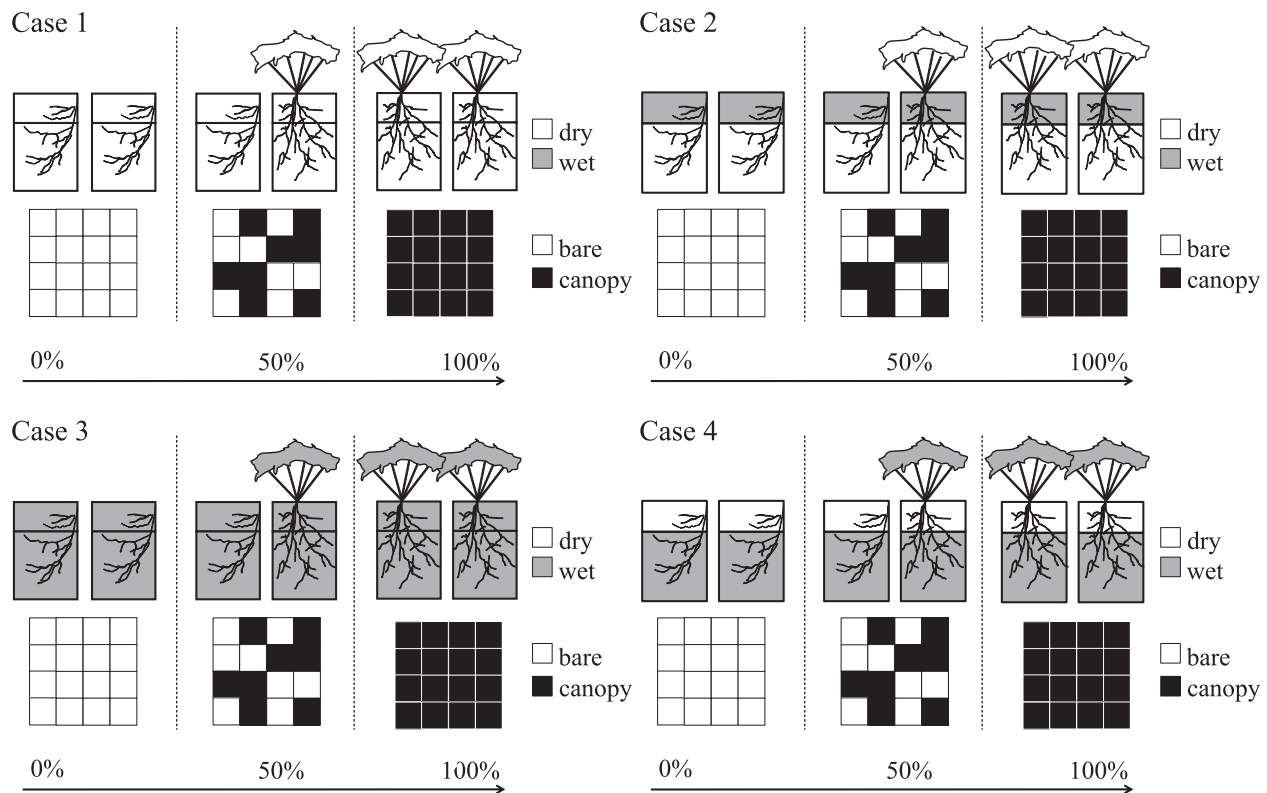


Figure 6. Visual representation of the virtual landscape showing Cases 1–4 and change in vegetation cover from 0% canopy to 100% canopy, using 0, 50, and 100% canopy cover as examples.

$$I_g = \frac{(2Green - Red - Blue)}{255} \quad (5)$$

where *Green* is the average green intensity of the ROI, *Red* is the average red intensity, and *Blue* is the average blue intensity. We then calculate a daily I_g for the study site by averaging the I_g from all three phenocams [Kurc and Benton, 2010]. It should be noted that daily I_g data are limited to 2011 due to theft of these cameras from the field site in 2012.

2.4. Remotely Sensed Albedo and Vegetation Data

For pixels located within the creosotebush-dominated region of the northern boundary of the SRER (Figures 1a and 1b), we derived 500×500 m woody cover, albedo, and NDVI (Normalized Difference Vegetation Index) from remotely sensed data sources (Figure 7). Landscape averages were calculated using the 32 pixels surrounding the tower where creosotebush were the dominant vegetation type (Figures 1b and 7). MODIS (Moderate Resolution Imaging Spectroradiometer) Bidirectional Reflectance Distribution Function albedo (MCD43A, BRDF/Albedo product) was downloaded from Oak Ridge National Laboratory (ORNL; daac.ornl.gov) for day of year (DOY) 161 in 2010 and for all of 2011. For this study, we used the shortwave actual albedo which accounts for white (diffused bihemispherical) and black (direct beam directional hemispherical) albedo. We used shortwave actual albedo values because the wavelength measured by both of the sensors used in the field was $0.3\text{--}3 \mu\text{m}$. MODIS (NDVI; MOD13A1) was downloaded from reverb (reverb.echo.nasa.gov) for DOY 161 in 2010 and from ORNL for all of 2011. NAIP (National Agriculture Imagery Program) 1×1 m data were obtained from the Farm Service Agency (fsa.usda.gov) for DOY 161 in 2010. A binary vegetation/bare soil classification was performed on the NAIP imagery using CART (classification and regression tree analysis) [Belward and DeHoyos, 1987; Homer et al., 2004; RuleQuestResearch, 2011]. The binary classification was resampled to 500×500 m to match the MCD43A MODIS albedo pixel size.

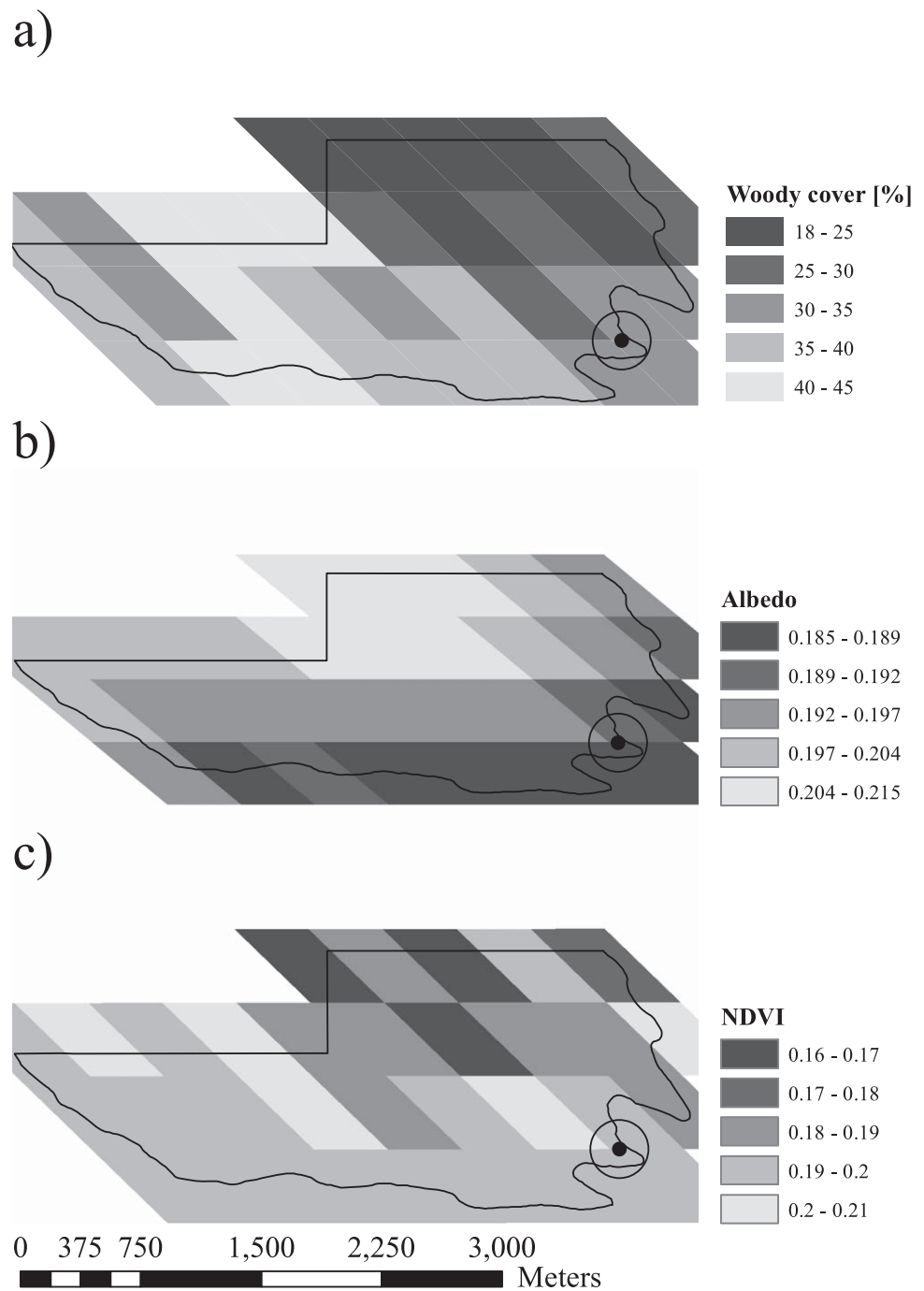


Figure 7. (a) Woody cover generated from NAIP data (2010, DOY 161), aggregation made at MODIS albedo pixel size (500×500 m), (b) MODIS albedo shortwave actual (2010, DOY 161), and (c) MODIS NDVI (2010, DOY 161). The EC tower is indicated with a dot, and the circle represents the tower footprint. The polygon demarcates the area prescribed by soil type to be dominated by creosotebush; however, personal experience indicates that the creosotebush ecosystem extends beyond this boundary.

3. Results and Discussion

Here we provide insight on how soil moisture present or absent in shallow or deep soil layers influences land surface albedo and suggest how this is modulated by the vegetation. We do this by analyzing (1) vegetation greenness derived from pheno-cam and remotely sensed images, (2) bare and canopy patch scale albedo in the context of our two-layer conceptual framework (Figure 2), (3) the influence of woody cover on

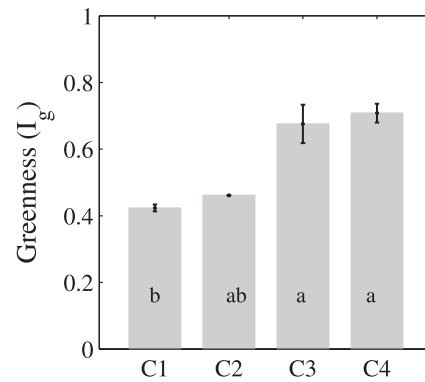


Figure 8. Bar graph of average greenness (I_g) computed from daily 2011 pheno-cam images that were categorized using two-layer soil moisture conceptual framework; Case 1 ($n = 227$), Case 2 ($n = 5$), Case 3 ($n = 17$), Case 4 ($n = 59$), no data ($n = 57$). Statistically significant differences between Cases derived from t-test (confidence interval = 0.95, p -value < 0.001) are indicated using different letters (a, b, and where ab is not significantly different from a or b, but would be significantly different than c).

albedo at a landscape scale using remotely sensed data, and (4) changes in albedo based on cover changes in a virtual landscape based on the two-layer conceptual framework (Figure 6).

3.1. Soil Moisture Influence on Greenness

As hypothesized, we found the canopies of the shrubs to be the greenest (i.e., highest I_g) when soil moisture was present in the deep layer (Cases 3 and 4) (Figure 8). Despite the fact that creosotebush is an evergreen shrub, change in greenness is observable (Figures 4 and 9a) because of changes in LAI (leaf area index) [Migliavacca et al., 2011] associated with moisture in the deep layer that triggers vegetation processes regardless of where the root density is highest [Cavanaugh et al., 2011; Kurc and Small, 2007; Kurc and Benton, 2010]. While I_g in Case 4 (mean = 0.71) was not significantly different than Case 3 (mean = 0.67), there was higher variability in Case 4 (Figure 8) that could be associated with meteorological conditions such as cloudiness [Migliavacca et al., 2011] and the complex interaction at the intercanopy level [Baldochi et al.,

1984; Eck and Deering, 1992]. Because Case 4 tended to follow Case 3 (e.g., Figure 3c), how moisture in the deep layer sustains canopy characteristics at the surface [e.g., Eastham et al., 1984; Ezcurra et al., 1992; Monson and Smith, 1982; Neufeld et al., 1988; Ong et al., 1985] must be considered.

While moisture is available in the shallow layer in Case 2, this moisture leaves the shallow layer quickly (Figure 10) [Jackson et al., 1976; Kurc and Small, 2004], presumably before the shrubs are able to use it [Kurc and Small, 2007]. Therefore, it is not surprising that I_g was lowest for Cases when moisture was absent from the deep layer (Cases 1 and 2) (Figure 8). This finding confirms our hypothesis that the canopy is perceived as drier when deep soil moisture is low and is consistent with a response mechanism to drought in which evergreen desert shrubs shed leaves [Hamerlynck and Huxman, 2009]. An alternative mechanism for the lower I_g in Case 1 than in Case 2 could be a result of canopy-litter interactions [van Leeuwen and Huete,

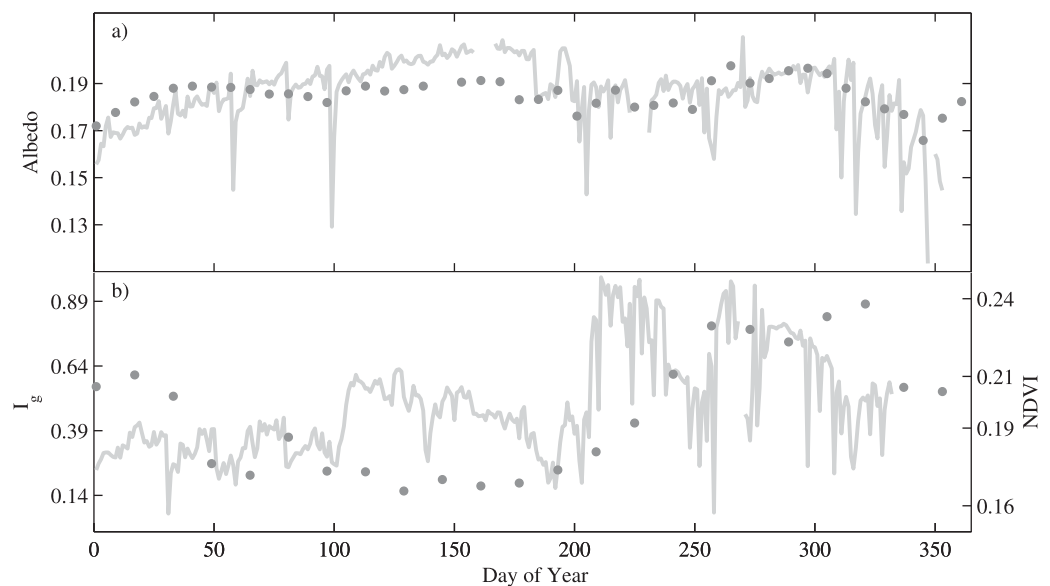


Figure 9. Time series of (a) greenness index (I_g) shown with thick gray line and MODIS NDVI average for the region shown with dark gray circles and (b) albedo values from EC flux tower with thick gray line and MODIS shortwave albedo average for the region shown with dark gray circles. Data correspond to 2011.

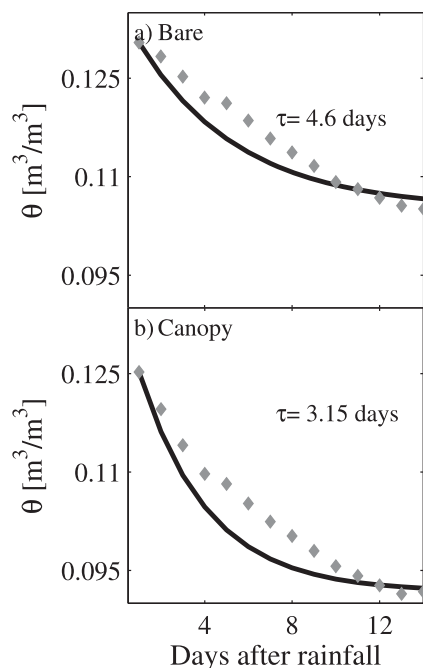


Figure 10. Drydown curves for shallow soil moisture from (a) bare and (b) canopy patches. The symbols indicate measurements, the line is an exponential fit, and τ is the exponential time constant.

1996] that result from the physical removal of leaves during precipitation events that led to the moisture in Case 2. Overall, these results support the differences between Cases when moisture is present in the deep layer (Cases 3 and 4) and Cases when moisture is absent in the deep layer (Cases 1 and 2) with respect to the canopy portion of our two-layer conceptual framework (Figure 2a).

At the larger scale, average NDVI for the 32 pixel landscape is 0.1914, with higher NDVI values in the pixels surrounding the tower (Figure 7c), suggestive of a landscape with higher vegetation cover in the northern portion of the landscape (Figure 7a). Increase in landscape NDVI (Figure 9a) appears to be associated with summer monsoon soil moisture (Figures 3a and 3b). While tower-based l_g also increases with summer monsoon moisture, two summer peaks are evident, suggesting that NDVI may not be sensitive enough to capture landscape scale vegetation dynamics that may influence land-surface atmosphere interactions. Furthermore, l_g also peaks slightly in the spring (Figure 9a), associated with small spring rainstorms (Figures 3a and 3b), which is also not captured within the NDVI time series. This is consistent with other findings that show that NDVI does not capture the carbon uptake dynamics or the associated changes in greenness of these sparse dryland ecosystems as well as pheno-cams do [Kurc and Benton, 2010].

3.2. Soil Moisture Influence on Albedo

Ecosystem albedo from the EC tower (section 2.2.2) varies throughout the year with an increase during the dry period (~DOY 100 to DOY 180) and a decrease around the monsoon season (Figure 9b). Ecosystem albedo was highest ($\alpha = 0.205$) when the entire soil profile was dry (Case 1), and in general albedo was higher for Cases when soil moisture was absent from the shallow layer (Cases 1 and 4) than when the shallow layer was wet (Cases 2 and 3) (Figure 11a). Lower land surface albedo is expected when the surface soil is wet [Fritschen, 1967; Small and Kurc, 2003; Twomey et al., 1986], so this is not surprising. Land surface albedo is influenced by the presence of vegetation [Idso, 1972], and therefore, we suspect that ecosystem albedo for Case 4 ($\alpha = 0.192$) was lower than for Case 1 because the shrubs were accessing deep moisture available in Case 4 and changing their reflectivity through greening [Kurc and Benton, 2010].

We hypothesized that bare albedo values for Cases when the shallow layer was dry (Cases 1 and 4) would be similar, and that values for Cases when the shallow layer was wet (Cases 2 and 3) would be similar (Figure 2b). However, while bare albedo values were highest for Cases 1 ($\alpha = 0.249$) and 4 ($\alpha = 0.220$) (Figure 11b), the albedo values were statistically different. This suggests that the surface characteristics in Case 4

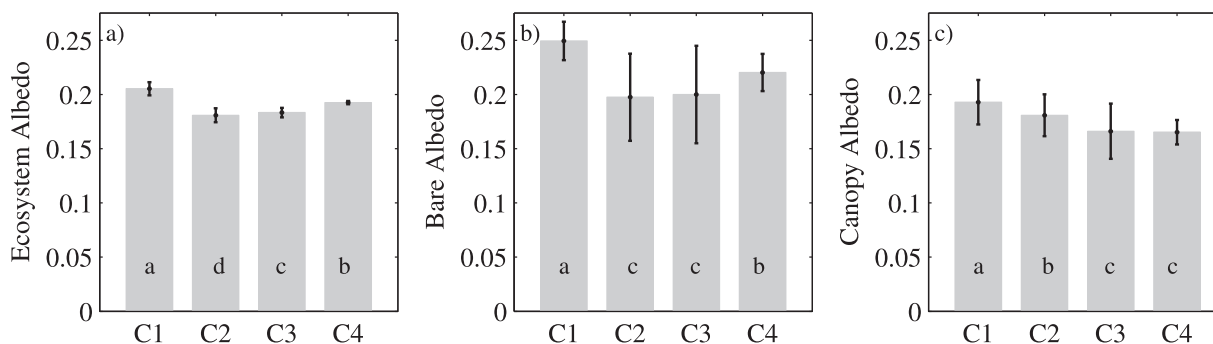


Figure 11. Bar graphs of average (a) ecosystem albedo (n = 16), (b) bare albedo (n = 128), and (c) canopy albedo (n = 128) for each Case (C1, Case 1; C2, Case 2; C3, Case 3; and C4, Case 4). Statistically significant differences between Cases derived from t-test (confidence interval = 0.95, p-value < 0.001) are indicated using different letters (a–d).

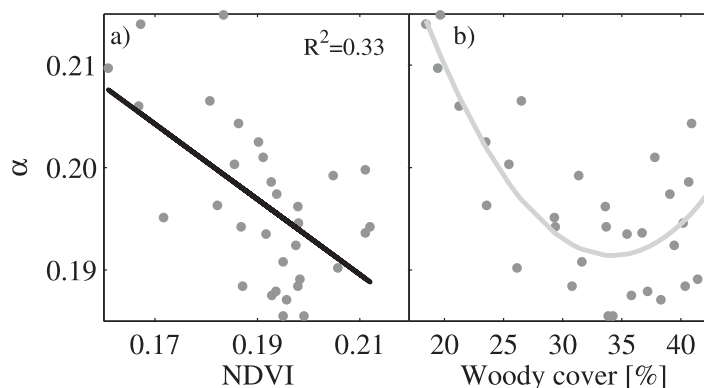


Figure 12. Relationship (a) between albedo (α) and NDVI at 500×500 m scale, and (b) between albedo and woody cover at 500×500 m scale. The R^2 values are for the linear regression.

differ from those in Case 1. We suspect this is through the presence of litter in Case 4 (that accumulates in the bare patches with overland flow after rainfall events) which is not as prevalent in Case 1 (Table 1).

When evaluating albedo for canopy patches, we expected that the albedo values for Cases when the deep layer was wet (Cases 3 and 4) would be comparably lower than the albedo values for Cases when the deep layer was dry (Cases 1 and 2) (Figure 2b), indicative of the influence of deep soil moisture on shrub canopy greenness. In fact, when evaluated for canopy patches, albedo values were lowest and statistically similar for Cases 3 ($\alpha = 0.166$) and 4 ($\alpha = 0.165$) despite their differences in shallow moisture (Figure 11c). Canopy albedo for Cases 3 and 4 were significantly different from Cases 1 ($\alpha = 0.193$) and 2 ($\alpha = 0.181$) (Figure 11c). In addition, Cases 1 and 2 had a sparser canopy than Cases 3 and 4 (Figure 4), resulting in a complex canopy-bare soil interaction. Because of this complex interaction, we suspect that albedo from Case 2 appears significantly lower than in Case 1, mostly because of the influence of the wet soil below the canopy.

As expected, albedo is always highest when both the shallow and deep layers are dry (Case 1) (Figures 11a–11c). Under these conditions, both the soil and the vegetation tend to be lighter in color (Figures 4 and 8, Table 1) and therefore more reflective. In Case 1, albedo is higher in the bare patches ($\alpha = 0.249$) than in the canopy patches ($\alpha = 0.193$) (Figures 11b and 11c). Ecosystem albedo calculated from tower data ($\alpha = 0.205$) falls between these values (Figure 11a), suggesting the influence of both bare and canopy albedo on the ecosystem.

Differences between albedo values from bare and canopy patches are largest for Cases when the shallow layer is dry (Cases 1 and 4) (Figures 11b and 11c), suggesting the presence of vegetation has the greatest influence on ecosystem albedo under dry surface soil conditions, despite the characteristics of the canopy (Figure 4). Albedo values from bare and canopy patches are most similar under Case 2 (Figures 11b and 11c), when the shallow layer is wet but the deep layer is dry. Under this condition, the vegetation is dry, light in color, with scarce leaves (Figure 4) [Kurc and Benton, 2010]. This suggests that the LAI of the vegetation is low enough so that the wet soil conditions pass through the canopy [van Leeuwen and Huete, 1996] and influence the shrub albedo signal [Asner, 1998].

The PDFs of bare albedo tend to be wider than PDFs of canopy albedo in Cases 2 and 3 (Figures 5b, 5c, 5f, and 5g), suggesting a combination of influences on albedo when shallow moisture is present. The PDFs of canopy albedo skew toward low values when moisture is present in the deep soil layers (Figures 5g and 5h).

3.3. Influence of Vegetation on Ecosystem Albedo via Access to Two-Layer Soil Moisture

In semiarid ecosystems, albedo values tend to be higher because of exposed bare ground [Charney, 1975; Otterman, 1974] and because moisture is lost quickly from this bare ground resulting in relatively more frequent light-colored surfaces [Jackson et al., 1976; Wythers et al., 1999]. We used a virtual landscape to investigate the role of increasing cover on ecosystem albedo in the presence or absence of soil moisture, changing vegetation cover by 10% increments from 0 to 100% (Figure 6), and calculating ecosystem albedo

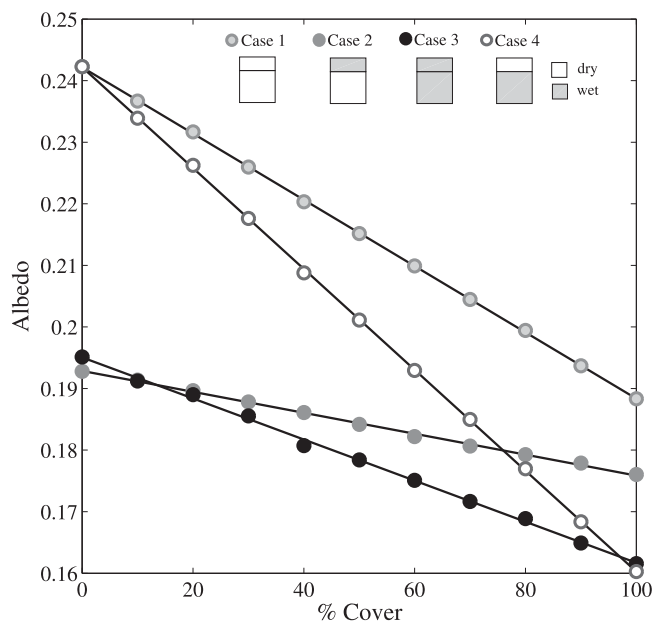


Figure 13. Virtual landscape outputs for change in canopy cover by 10% increments and corresponding changes in albedo for each soil moisture case.

(equation (4)) as an average of the patches within the grid. We expected that at 0% cover, our virtual landscape ecosystem albedo values for Cases 1 and 4 would be similar as would ecosystem albedo values for Cases 2 and 3, representing the conditions of the bare soil patches (Figure 6). When moisture was absent in the shallow layer but present in the deep layer (Case 4), we expected that as cover increased ecosystem albedo would converge toward the virtual landscape ecosystem albedo for Case 3. We expected this because the deep layer moisture is accessible by the vegetation under these conditions [Kirc and Small, 2007; Raz-Yaseef et al., 2012] creating wet and therefore dark canopies (Figures 4 and 8). Therefore, at 100% cover, the surface should appear dark in color,

regardless of the color of the soil below the canopy (Figure 6). Further, when moisture was present in the shallow layer but absent in the deep layer (Case 2), we expected that as cover increased virtual landscape ecosystem albedo would converge toward the ecosystem albedo for Case 1 because moisture is not accessible by the vegetation under these conditions, creating dry and therefore light canopies (Figures 4 and 8). Therefore, at 100% cover, the surface should appear light in color regardless of the color of the soil beneath it (Figure 6). Finally, we expected that the convergence of Case 4 to Case 3 should be stronger than the convergence of Case 2 to Case 1 because canopies present under the conditions of Cases 3 and 4 should have higher LAI because they are under less water stress. Therefore, the canopies in Cases 3 and 4 should have less influence from the soil beneath the canopy than Cases 1 and 2.

Increasing cover resulted in the largest change in virtual landscape ecosystem albedo ($\sim 8\%$ decrease) for Case 4 (a dry shallow layer and a wet deep layer) (Figure 13). This result suggests that at this site, the albedo of wet vegetation with high I_g (Figure 8) is very different than the albedo of dry surface soil (Figure 13). Case 1 also underwent a large decrease in ecosystem albedo with increasing cover ($\sim 5\%$), becoming more similar to Case 2 (Figure 13), as expected. The smallest change in ecosystem albedo with increasing cover ($\sim 2\%$) occurred when the shallow layer was wet but the deep layer was dry (Case 2). This suggests that, at least at this site, the albedo of dry vegetation (Figure 4) with low I_g (Figure 8) is more similar to the albedo of wet surface soil than to the albedo of dry surface soil.

As expected, the albedo values for Cases 3 and 4 converged with increasing cover (Figure 13). In fact, the ecosystem albedo for Case 4 was nearly identical to the ecosystem albedo for Case 3 after cover was increased to 100%, supporting the hypothesis that the canopies sufficiently cover the soil surface under these conditions such that the ecosystem albedo is not influenced by it. While the albedo values of Cases 1 and 2 also began to converge when cover was increased from 0 to 100%, ecosystem albedo for Cases 1 and 2 were still quite different (Figure 13). This difference was nearly as large as the difference between Cases 2 and 3 at 100% cover. This supports the notion that the canopies do not sufficiently cover the soil surface under these conditions and therefore the ecosystem albedo is still influenced by the soil surface. Finally, according to our virtual landscape experiment, albedo values for Cases 2 and 3 should look identical at around 30% cover (Figure 13). Additionally, albedo values for Cases 2 and 4 should look identical at around 75% cover (Figure 13).

The virtual landscape in this study dictates that increases in vegetation cover influence albedo linearly (Figure 13), similar to what Ge and Zou [2013] suggest. However, the natural system is much more complex

[Asbjornsen *et al.*, 2011; Wang *et al.*, 2012]. For instance, the virtual landscape albedo for Case 1 at 24% cover is 0.228 (and at 14% cover is 0.235). On DOY 158 in 2010 (no data from 159 to 175), when the actual ecosystem was in Case 1, the ecosystem albedo calculated from the tower was 0.203, where percent shrub cover is 14% (section 2.1). On DOY 161, MODIS albedo for the single pixel surrounding the tower was 0.186 (% woody cover = 34), while the 32 pixel landscape average is 0.196 (% woody cover = 32). While albedo decreases with increasing woody cover across these estimates, the differences in albedo between methods highlight the uncertainty associated with different temporal and spatial scales. This uncertainty is important to consider in the parameterization of land surface models, especially when considering interactions between soil moisture and vegetation.

Using MODIS data for DOY 161, 2010 which falls in our Case 1 (dry/dry), we show that increases in NDVI in this landscape results in a decrease in albedo (Figure 12a). NAIP data for DOY 161, 2010 suggest that the landscape surrounding the EC tower ranges from 18 to 45% woody cover (Figure 12b), with an average of 32% cover, resulting in an average landscape albedo of 0.196. Interestingly, in this landscape, the effect of decreasing albedo with increasing woody cover on albedo peaks at mid ranges of cover (30–35%), before albedo begins to increase again (Figure 12b). We suspect this could be the result of the more dense vegetation competing for sparse water, which effectively dries and lightens the canopy. This is an important consideration in land surface modeling applications where, at least for semiarid ecosystems, changes in albedo may not be linearly related to changes in vegetative cover.

3.4. Implications of Soil Moisture Drydown Differences Between Bare and Canopy Patches

Based on previous studies [Boulet *et al.*, 2004; Kurc and Small, 2004; Liou *et al.*, 1998], we expected that the length of time that a bare and canopy patch remained in each Case would be different and that these differences would have implications for land-atmosphere modeling applications that identify bare and canopy patches within a two-layer soil moisture framework. In particular, we expected evaporation to be higher in bare patches [Villegas *et al.*, 2010b] so that bare patches would remain in Cases 2 and 3 for less time than canopy patches.

Interestingly, we found that the shallow layers of canopy patches actually dried more quickly (Figure 8b; $\tau = 3.15$ days) than the shallow layers of bare patches (Figure 8a; $\tau = 4.6$ days), by more than one full day. This suggests that contrary to our initial expectation, bare patches would remain in Cases 2 and 3 longer than canopy patches would. Infiltration is expected to be higher under canopy patches than under bare patches [Bhark and Small, 2003] due in part to increased interception and stemflow [e.g., Reynolds *et al.*, 1999], and the movement of moisture belowground through root macropores [e.g., Mitchell *et al.*, 1995]. Evaporation from these canopy shallow layers may be large relative to bare shallow layers because of larger pore spaces in the soil beneath the canopy or compaction of soil in the bare patches.

4. Conclusions

The results from our study show that canopy greenness in a semiarid shrub ecosystem is triggered by deep soil moisture. In our evergreen shrubland, the difference in greenness between dry conditions (Cases 1 and 2) and wet conditions (Cases 3 and 4) is about 40%. By triggering greenness, deep soil moisture also decreases canopy albedo (e.g., the difference between Cases 1 and 4 is about 14%). This suggests that deep soil moisture has an important role in semiarid land-atmosphere interactions. In particular, deep soil moisture can affect the physical surface energy dynamics, and the understanding of these processes has implications for modeling [Niyogi *et al.*, 1997, 1999; Sanchez-Mejia and Papuga, 2014; Santanello *et al.*, 2005, 2013; Zaitchik *et al.*, 2013]. This is especially important in semiarid ecosystems, which are largely confined to the water-limited conditions, rather than energy-limited conditions, that influence evapotranspiration dynamics [Jackson *et al.*, 1976], in addition to other land-atmosphere exchanges. In these semiarid ecosystems, moisture only moves below a shallow surface layer after large rainfall events or series of smaller events [Kurc and Small, 2007]. While future climate predictions indicate that total precipitation is likely to continue decreasing in semiarid areas [e.g., Woodhouse *et al.*, 2010], whether this reduced precipitation arrives as smaller rainfall events or more infrequent large rainfall events will have important consequences for vegetation [Heisler-White *et al.*, 2008; Huxman *et al.*, 2004] and therefore the partitioning of

energy in these ecosystems. These changes will result in further feedbacks with the climate system [e.g., *Notaro et al.*, 2006; *Penuelas et al.*, 2009].

Acknowledgments

This research was supported in part by The University of Arizona College of Agriculture and Life Sciences (CALIS), The Arizona University System Technology and Research Initiative Fund (TRIF), The University of Arizona Office of the Vice President for Research (VPR), SAHRA (Sustainability of semi-Arid Hydrology and Riparian areas) under the STC Program of the National Science Foundation (NSF), NSF CAREER Award # EAR-1255013, and a doctoral studies fellowship provided through Mexican National Council for Science and Technology (CONACYT). Data associated with this manuscript can be obtained by contacting the corresponding author. Patch scale shortwave radiation measurements were made possible through field equipment provided by Dr. Russell Scott. Additional field assistance for the campaign measurements was provided by Lori Lovell, Evan Kipnis, Krystine Nelson, and Daniel Bunting. This manuscript benefited greatly from the helpful comments of Steve Archer, Xubin Zeng, Francina Dominguez, and two anonymous reviewers.

References

- Archer, S. (1990), Development and stability of grass woody mosaics in subtropical savanna parkland, Texas, USA, *J. Biogeogr.*, *17*(4–5), 453–462.
- Arriaga, F. J., B. Lowery, and M. D. Mays (2006), A fast method for determining soil particle size distribution using a laser instrument, *Soil Sci.*, *171*(9), 663–674.
- Asbjornsen, H., et al. (2011), Ecohydrological advances and applications in plant-water relations research: A review, *J. Plant Ecol.*, *4*(1–2), 3–22.
- Asner, G. P. (1998), Biophysical and biochemical sources of variability in canopy reflectance, *Remote Sens. Environ.*, *64*(3), 234–253.
- Asner, G. P., S. Archer, R. F. Hughes, R. J. Ansley, and C. A. Wessman (2003), Net changes in regional woody vegetation cover and carbon storage in Texas Drylands, 1937–1999, *Global Change Biol.*, *9*(3), 316–335.
- Austin, A., L. Yahdjian, J. Stark, J. Belnap, A. Porporato, U. Norton, D. Ravetta, and S. Schaeffer (2004), Water pulses and biogeochemical cycles in arid and semiarid ecosystems, *Oecologia*, *141*(2), 221–235.
- Baldocchi, D., D. Matt, B. Hutchison, and R. McMillen (1984), Solar-radiation within an oak hickory forest—An evaluation of the extinction coefficients for several radiation components during fully-leaved and leafless periods, *Agric. For. Meteorol.*, *32*(3–4), 307–322.
- Baldocchi, D., L. Xu, and N. Kiang (2004), How plant functional-type, weather, seasonal drought, and soil physical properties alter water and energy fluxes of an oak-grass savanna and an annual grassland, *Agric. For. Meteorol.*, *123*(1–2), 13–39.
- Baldocchi, D., T. Krebs, and M. Leclerc (2005), "Wet/dry Daisyworld": A conceptual tool for quantifying the spatial scaling of heterogeneous landscapes and its impact on the subgrid variability of energy fluxes, *Tellus, Ser. B*, *57*(3), 175–188.
- Basara, J. B., and K. C. Crawford (2002), Linear relationships between root-zone soil moisture and atmospheric processes in the planetary boundary layer, *J. Geophys. Res.*, *107*(D15), 4274, doi:10.1029/2001JD000633.
- Belward, A., and A. DeHoyos (1987), A comparison of supervised maximum-likelihood and decision tree classification for crop estimation from multitemporal LANDSAT MSS data, *Int. J. Remote Sens.*, *8*(2), 229–235.
- Bhark, E., and E. Small (2003), Association between plant canopies and the spatial patterns of infiltration in shrubland and grassland of the Chihuahuan Desert, New Mexico, *Ecosystems*, *6*(2), 185–196.
- Bonan, G. B., S. Levis, S. Sitch, M. Vertenstein, and K. W. Oleson (2003), A dynamic global vegetation model for use with climate models: Concepts and description of simulated vegetation dynamics, *Global Change Biol.*, *9*(11), 1543–1566.
- Boulet, G., A. Chehbouni, I. Braud, B. Duchemin, and A. Lakhal (2004), Evaluation of a two-stage evaporation approximation for contrasting vegetation cover, *Water Resour. Res.*, *40*, W12507, doi:10.1029/2004WR003212.
- Breshears, D. D., and F. J. Barnes (1999), Interrelationships between plant functional types and soil moisture heterogeneity for semiarid landscapes within the grassland/forest continuum: A unified conceptual model, *Landsc. Ecol.*, *14*(5), 465–478.
- Carrion, J. S., S. Fernandez, G. Jimenez-Moreno, S. Fauquette, G. Gil-Romera, P. Gonzalez-Samperiz, and C. Finlayson (2010), The historical origins of aridity and vegetation degradation in southeastern Spain, *J. Arid Environ.*, *74*(7), 731–736.
- Cavanaugh, M., S. Kurc, and R. Scott (2011), Evapotranspiration partitioning in semiarid shrubland ecosystems: A two-site evaluation of soil moisture control on transpiration, *Ecohydrology*, *4*(5), 671–681.
- Cescatti, A., et al. (2012), Intercomparison of MODIS albedo retrievals and in situ measurements across the global FLUXNET network, *Remote Sens. Environ.*, *121*, 323–334.
- Charney, J. (1975), Dynamics of deserts and drought in the Sahel, *Q. J. R. Meteorol. Soc.*, *101*(428), 193–202.
- Colwell, J. (1974), Vegetation canopy reflectance, *Remote Sens. Environ.*, *3*(3), 175–183.
- Duchon, C. E., and K. G. Hamm (2006), Broadband albedo observations in the southern Great Plains, *J. Appl. Meteorol. Climatol.*, *45*(1), 210–235.
- Eastham, J., D. M. Oosterhuis, and S. Walker (1984), Leaf water and turgor potential threshold values for leaf growth of wheat, *Agron. J.*, *76*(5), 841–847.
- Eck, T., and D. Deering (1992), Canopy albedo and transmittance in a spruce-hemlock forest in mid-September, *Agric. For. Meteorol.*, *59*(3–4), 237–248.
- Ezcurra, E., S. Arizaga, P. L. Valverde, C. Mourelle, and A. Floresmartinez (1992), Foliolate movement and canopy architecture of *Larrea tridentata* (DC) Cov in Mexican deserts, *Oecologia*, *92*(1), 83–89.
- Fritschen, L. J. (1967), Net and solar radiation relations over irrigated field crops, *Agric. Meteorol.*, *4*(1), 55–62.
- Ge, J., and C. Zou (2013), Impacts of woody plant encroachment on regional climate in the southern Great Plains of the United States, *J. Geophys. Res.*, *118*, 9093–9104, doi:10.1002/jgrd.50634.
- Grover, H. D., and H. B. Musick (1990), Shrubland encroachment in southern New Mexico, U.S.A.: An analysis of desertification processes in the American southwest, *Clim. Change*, *17*(2–3), 305–330.
- Gu, L. H., et al. (2007), Influences of biomass heat and biochemical energy storages on the land surface fluxes and radiative temperature, *J. Geophys. Res.*, *112*, D02107, doi:10.1029/2006JD007425.
- Hamerlynck, E. P., and T. E. Huxman (2009), Ecophysiology of two Sonoran Desert evergreen shrubs during extreme drought, *J. Arid Environ.*, *73*(4–5), 582–585.
- Heisler-White, J. L., A. K. Knapp, and E. F. Kelly (2008), Increasing precipitation event size increases aboveground net primary productivity in a semi-arid grassland, *Oecologia*, *158*(1), 129–140.
- Homer, C., C. Huang, L. Yang, B. Wylie, and M. Coan (2004), Development of a 2001 National Landcover Database for the United States, *Photogramm. Eng. Remote Sens.*, *70*(7), 829–840.
- Hunt, J. E., F. M. Kelliher, T. M. McSeveny, and J. N. Byers (2002), Evaporation and carbon dioxide exchange between the atmosphere and a tussock grassland during a summer drought, *Agric. For. Meteorol.*, *111*(1), 65–82.
- Huxman, T. E., K. A. Snyder, D. Tissue, A. J. Leffler, K. Ogle, W. T. Pockman, D. R. Sandquist, D. L. Potts, and S. Schwinning (2004), Precipitation pulses and carbon fluxes in semiarid and arid ecosystems, *Oecologia*, *141*(2), 254–268.
- Idso, S. B. (1972), A note on some recently proposed mechanisms of genesis of deserts, *Q. J. R. Meteorol. Soc.*, *103*(436), 369–370.
- Jackson, R., S. Idso, and R. Reginato (1976), Calculation of evaporation rates during the transition from energy-limiting to soil-limiting phases using albedo data, *Water Resour. Res.*, *12*(1), 23–26.
- Jackson, R., et al. (2000), Belowground consequences of vegetation change and their treatment in models, *Ecol. Appl.*, *10*(2), 470–483.

- Krinner, G., N. Viovy, N. de Noblet-Ducoudre, J. Ogee, J. Polcher, P. Friedlingstein, P. Ciais, S. Sitch, and I. C. Prentice (2005), A dynamic global vegetation model for studies of the coupled atmosphere-biosphere system, *Global Biogeochem. Cycles*, *19*, GB1015, doi:10.1029/2003GB002199.
- Kurc, S., and L. Benton (2010), Digital image-derived greenness links deep soil moisture to carbon uptake in a creosotebush-dominated shrubland, *J. Arid Environ.*, *74*(5), 585–594.
- Kurc, S., and E. Small (2004), Dynamics of evapotranspiration in semiarid grassland and shrubland ecosystems during the summer monsoon season, central New Mexico, *Water Resour. Res.*, *40*, W09305, doi:10.1029/2004WR003068.
- Kurc, S., and E. Small (2007), Soil moisture variations and ecosystem-scale fluxes of water and carbon in semiarid grassland and shrubland, *Water Resour. Res.*, *43*, W06416, doi:10.1029/2006WR005011.
- Liang, X., et al. (2005), Development of land surface albedo parameterization based on Moderate Resolution Imaging Spectroradiometer (MODIS) data, *J. Geophys. Res.*, *110*, D11107, doi:10.1029/2004JD005579.
- Liou, Y. A., E. J. Kim, and A. W. England (1998), Radiobrightness of prairie soil and grassland during dry-down simulations, *Radio Sci.*, *33*(2), 259–265.
- Lobell, D., and G. Asner (2002), Moisture effects on soil reflectance, *Soil Sci. Soc. Am. J.*, *66*(3), 722–727.
- Lohmann, D., and E. F. Wood (2003), Timescales of land surface evapotranspiration response in the PILPS phase 2(c), *Global Planet. Change*, *38*(1–2), 81–91.
- Loik, M. E., D. D. Breshears, W. K. Lauenroth, and J. Belnap (2004), A multi-scale perspective of water pulses in dryland ecosystems: Climatology and ecohydrology of the western USA, *Oecologia*, *141*(2), 269–281.
- Lucht, W., A. H. Hyman, A. H. Strahler, M. J. Barnsley, P. Hobson, and J. P. Muller (2000), A comparison of satellite-derived spectral albedos to ground-based broadband albedo measurements modeled to satellite spatial scale for a semidesert landscape, *Remote Sens. Environ.*, *74*(1), 85–98.
- Mahrt, L., and H. Pan (1984), A 2-layer model of soil hydrology, *Boundary Layer Meteorol.*, *29*(1), 1–20.
- Mendez-Barroso, L. A., E. R. Vivoni, C. J. Watts, and J. C. Rodriguez (2009), Seasonal and interannual relations between precipitation, surface soil moisture and vegetation dynamics in the North American monsoon region, *J. Hydrol.*, *377*(1–2), 59–70.
- Migliavacca, M., et al. (2011), Using digital repeat photography and eddy covariance data to model grassland phenology and photosynthetic CO₂ uptake, *Agric. For. Meteorol.*, *151*(10), 1325–1337.
- Mitchell, A. R., T. R. Ellsworth, and B. D. MEEK (1995), Effect of root systems on preferential flow in swelling soil, *Commun. Soil Sci. Plant Anal.*, *26*(15–16), 2655–2666.
- Monson, R. K., and S. D. Smith (1982), Seasonal water potential components of Sonoran Desert plants, *Ecology*, *63*(1), 113–123.
- Moody, A., and R. K. Meentemeyer (2001), Environmental factors influencing spatial patterns of shrub diversity in chaparral, Santa Ynez Mountains, California, *J. Veg. Sci.*, *12*(1), 41–52.
- Neufeld, H. S., F. C. Meinzer, C. S. Wisdom, M. R. Sharifi, P. W. Rundel, M. S. Neufeld, Y. Goldring, and G. L. Cunningham (1988), Canopy architecture of *Larrea tridentata* (DC) Cov, a desert shrub—Foliage orientation and direct beam radiation interception, *Oecologia*, *75*(1), 54–60.
- Nicholson, S. E. (2000), Land surface processes and Sahel climate, *Rev. Geophys.*, *38*(1), 117–139.
- Nicholson, S. E., C. J. Tucker, and M. B. Ba (1998), Desertification, drought, and surface vegetation: An example from the West African Sahel, *Bull. Am. Meteorol. Soc.*, *79*(5), 815–829.
- Niyogi, D., S. Raman, and K. Alapaty (1999), Uncertainty in the specification of surface characteristics, part II: Hierarchy of interaction-explicit statistical analysis, *Boundary Layer Meteorol.*, *91*(3), 341–366.
- Niyogi, D., S. Raman, K. Alapaty, and J. Han (1997), A dynamic statistical experiment for atmospheric interactions, *Environ. Model. Assess.*, *2*(4), 307–322.
- Notaro, M., Z. Liu, and J. W. Williams (2006), Observed vegetation-climate feedbacks in the United States, *J. Clim.*, *19*(5), 763–786.
- Noy-Meir, I. (1973), Desert ecosystems: Environment and producers, *Annu. Rev. Ecol. Syst.*, *4*, 25–51.
- Ong, C. K., C. R. Black, L. P. Simmonds, and R. A. Saffell (1985), Influence of saturation deficit on leaf production and expansion in stands of groundnut (*arachis hypogaea* l) grown without irrigation, *Ann. Bot.*, *56*(4), 523–536.
- Otterman, J. (1974), Baring high-albedo soils by overgrazing—Hypothesized desertification mechanism, *Science*, *186*(4163), 531–533.
- Otterman, J. (1977), Monitoring surface albedo change with LANDSAT, *Geophys. Res. Lett.*, *4*(10), 441–444.
- Overpeck, J., and B. Udall (2010), Dry times ahead, *Science*, *328*(5986), 1642–1643.
- Partel, M., and A. Helm (2007), Invasion of woody species into temperate grasslands: Relationship with abiotic and biotic soil resource heterogeneity, *J. Veg. Sci.*, *18*(1), 63–70.
- Penuelas, J., T. Rutishauser, and I. Filella (2009), Phenology feedbacks on climate change, *Science*, *324*(5929), 887–888.
- Philippon, N., E. Mougou, L. Jarlan, and P. L. Frison (2005), Analysis of the linkages between rainfall and land surface conditions in the West African monsoon through CMAP, ERS-WSC, and NOAA-AVHRR data, *J. Geophys. Res.*, *110*, D24115, doi:10.1029/2005JD006394.
- Raz-Yaseef, N., D. Yakir, G. Schiller, and S. Cohen (2012), Dynamics of evapotranspiration partitioning in a semi-arid forest as affected by temporal rainfall patterns, *Agric. For. Meteorol.*, *157*, 77–85.
- Reynolds, J. F., R. A. Virginia, P. R. Kemp, A. G. de Soya, and D. C. Tremmel (1999), Impact of drought on desert shrubs: Effects of seasonality and degree of resource island development, *Ecol. Monogr.*, *69*(1), 69–106.
- Richardson, A. D., J. P. Jenkins, B. H. Braswell, D. Y. Hollinger, S. V. Ollinger, and M. L. Smith (2007), Use of digital webcam images to track spring green-up in a deciduous broadleaf forest, *Oecologia*, *152*(2), 323–334.
- Roberts, D. A., S. L. Ustin, S. Ogunjemiyo, J. Greenberg, S. Z. Dobrowski, J. Q. Chen, and T. M. Hinckley (2004), Spectral and structural measures of northwest forest vegetation at leaf to landscape scales, *Ecosystems*, *7*(5), 545–562.
- Robinove, C., P. Chavez, D. Gehring, and R. Holmgren (1981), Arid land monitoring using LANDSAT albedo difference images, *Remote Sens. Environ.*, *11*(2), 133–156.
- Rodriguez-Iturbe, I. (2000), Ecohydrology: A hydrologic perspective of climate-soil-vegetation dynamics, *Water Resour. Res.*, *36*(1), 3–9.
- Rodriguez-Iturbe, I., P. D'Odorico, A. Porporato, and L. Ridolfi (1999), On the spatial and temporal links between vegetation, climate, and soil moisture, *Water Resour. Res.*, *35*(12), 3709–3722.
- RuleQuestResearch (2011), *Data Mining Tools See5 and c5.0*, St Ives, RuleQuest Research, NSW, Australia.
- Sala, O., and W. Lauenroth (1982), Small rainfall events: An ecological role in semiarid regions, *Oecologia*, *53*(3), 301–304.
- Sanchez-Mejia, Z., and S. Papuga (2014), Observations of a two-layer soil moisture influence on surface energy dynamics and planetary boundary layer characteristics in a semiarid shrubland, *Water Resour. Res.*, *50*, 306–317, doi:10.1002/2013WR014135.
- Santanello, J., M. Friedl, and W. Kustas (2005), An empirical investigation of convective planetary boundary layer evolution and its relationship with the land surface, *J. Appl. Meteorol.*, *44*(6), 917–932.

- Santanello, J., C. Peters-Lidard, S. Kumar, C. Alonge, and W. Tao (2009), A modeling and observational framework for diagnosing local land-atmosphere coupling on diurnal time scales, *J. Hydrometeorol.*, *10*(3), 577–599.
- Santanello, J., C. Peters-Lidard, A. Kennedy, and S. Kumar (2013), Diagnosing the nature of land-atmosphere coupling: A case study of dry/wet extremes in the US Southern Great Plains, *J. Hydrometeorol.*, *14*(1), 3–24.
- Schaaf, C. B., Z. Wang, and A. H. Strahler (2011), Commentary on Wang and Zender-MODIS snow albedo bias at high solar zenith angles relative to theory and to in situ observations in Greenland, *Remote Sens. Environ.*, *115*(5), 1296–1300.
- Schwinnig, S., and O. Sala (2004), Hierarchy of responses to resource pulses in arid and semi-arid ecosystems, *Oecologia*, *141*(2), 211–220.
- Scott, R., D. Entekhabi, R. Koster, and M. Suarez (1997), Timescales of land surface evapotranspiration response, *J. Clim.*, *10*(4), 559–566.
- Seghier, J., S. Galle, J. L. Rajot, and M. Ehrmann (1997), Relationships between soil moisture and growth of herbaceous plants in a natural vegetation mosaic in Niger, *J. Arid Environ.*, *36*(1), 87–102.
- Siqueira, M., G. Katul, and A. Porporato (2009), Soil moisture feedbacks on convection triggers: The role of soil-plant hydrodynamics, *J. Hydrometeorol.*, *10*(1), 96–112.
- Small, E., and S. Kurc (2003), Tight coupling between soil moisture and the surface radiation budget in semiarid environments: Implications for land-atmosphere interactions, *Water Resour. Res.*, *39*(10), 1278, doi:10.1029/2002WR001297.
- Song, J. (1999), Phenological influences on the albedo of prairie grassland and crop fields, *Int. J. Biometeorol.*, *42*(3), 153–157.
- Swann, A., I. Fung, and J. Chiang (2012), Mid-latitude afforestation shifts general circulation and tropical precipitation, *Proc. Natl. Acad. Sci. U. S. A.*, *109*(3), 712–716.
- Thomey, M. L., S. L. Collins, R. Vargas, J. E. Johnson, R. F. Brown, D. O. Natvig, and M. T. Friggens (2011), Effect of precipitation variability on net primary production and soil respiration in a Chihuahuan Desert grassland, *Global Change Biol.*, *17*(4), 1505–1515.
- Twomey, S. A., C. F. Bohren, and J. L. Mergenthaler (1986), Reflectance and albedo differences between wet and dry surfaces, *Appl. Optics*, *25*(3), 431–437.
- Van Auken, O. W. (2000), Shrub invasions of North American semiarid grasslands, *Annu. Rev. Ecol. Syst.*, *31*, 197–215.
- van Leeuwen, W. J. D., and A. R. Huete (1996), Effects of standing litter on the biophysical interpretation of plant canopies with spectral indices, *Remote Sens. Environ.*, *55*(2), 123–138.
- Villegas, J. C., D. D. Breshears, C. B. Zou, and P. D. Royer (2010a), Seasonally pulsed heterogeneity in microclimate: Phenology and cover effects along deciduous grassland-forest continuum, *Vadose Zone J.*, *9*(3), 537–547.
- Villegas, J. C., D. D. Breshears, C. B. Zou, and D. J. Law (2010b), Ecohydrological controls of soil evaporation in deciduous drylands: How the hierarchical effects of litter, patch and vegetation mosaic cover interact with phenology and season, *J. Arid Environ.*, *74*(5), 595–602.
- Walter, H. (1972), *Ecology of Tropical and Subtropical Vegetation*, Oliver and Boyd, Edinburgh, U. K.
- Wang, G., Y. Kim, and D. Wang (2007), Quantifying the strength of soil moisture-precipitation coupling and its sensitivity to changes in surface water budget, *J. Hydrometeorol.*, *8*(3), 551–570.
- Wang, L., P. D'Odorico, J. Evans, D. Eldridge, M. McCabe, K. Caylor, and E. King (2012), Dryland ecohydrology and climate change: Critical issues and technical advances, *Hydrol. Earth Syst. Sci.*, *16*(8), 2585–2603.
- Wang, Y., M. Shao, Y. Zhu, and Z. Liu (2011), Impacts of land use and plant characteristics on dried soil layers in different climatic regions on the Loess Plateau of China, *Agric. For. Meteorol.*, *151*(4), 437–448.
- Wiegand, K., D. Saitz, and D. Ward (2006), A patch-dynamics approach to savanna dynamics and woody plant encroachment—Insights from an arid savanna, *Perspect. Plant Ecol. Evol. Syst.*, *7*(4), 229–242.
- Woodhouse, C. A., D. M. Meko, G. M. MacDonald, D. W. Stahle, and E. R. Cooke (2010), A 1,200-year perspective of 21st century drought in southwestern North America, *Proc. Natl. Acad. Sci. U. S. A.*, *107*(50), 21,283–21,288.
- Wu, A. H., Z. Q. Li, and J. Cihlar (1995), Effects of land-cover type and greenness on advanced very high-resolution radiometer bidirectional reflectances—Analysis and removal, *J. Geophys. Res.*, *100*(D5), 9179–9192.
- Wythers, K. R., W. K. Lauenroth, and J. M. Paruelo (1999), Bare-soil evaporation under semiarid field conditions, *Soil Sci. Soc. Am. J.*, *63*(5), 1341–1349.
- Zaitchik, B., J. Santanello, S. Kumar, and C. Peters-Lidard (2013), Representation of soil moisture feedbacks during drought in NASA unified WRF (NU-WRF), *J. Hydrometeorol.*, *14*(1), 360–367.
- Zhang, J., and J. Walsh (2006), Thermodynamic and hydrological impacts of increasing greenness in northern high latitudes, *J. Hydrometeorol.*, *7*(5), 1147–1163.
- Zhang, X., Q. Tang, J. Zheng, and Q. Ge (2013), Warming/cooling effects of cropland greenness changes during 1982–2006 in the North China Plain, *Environ. Res. Lett.*, *8*(2), 024038, doi:10.1088/1748-9326/8/2/024038.